Supporting information

Tae Hoon Ha, Jeong Yeol Yoo, Seung Wan Kang and Chil Won Lee*

Department of Chemistry, Dankook University, Cheonan 31116, Korea

***Corresponding author. Email: chili@dankook.ac.kr; Fax: +82-31-8021-7218.**

◆ [1]H and [13]C NMR spectra and GC-Mass data

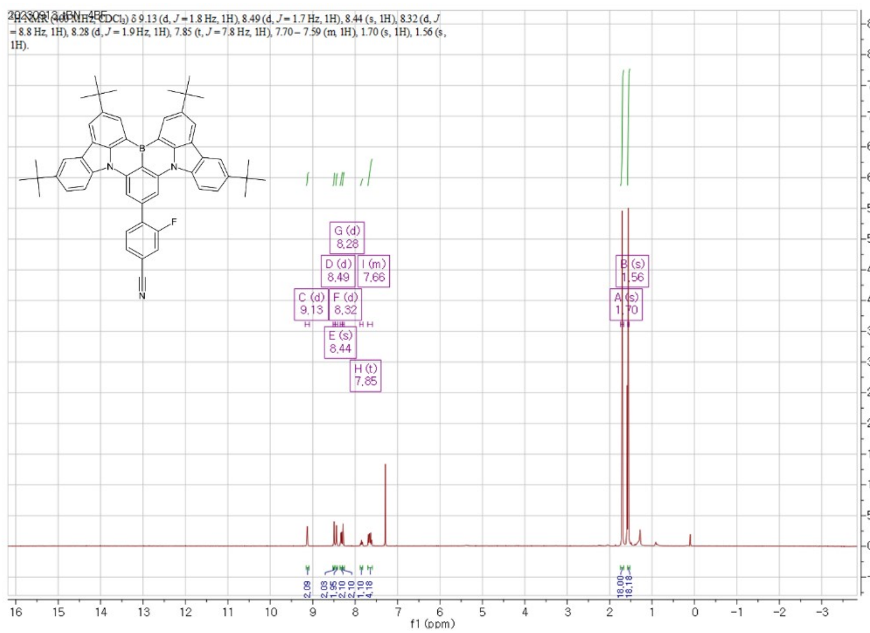

Fig. S1. [1]H-NMR of tBN-4BF

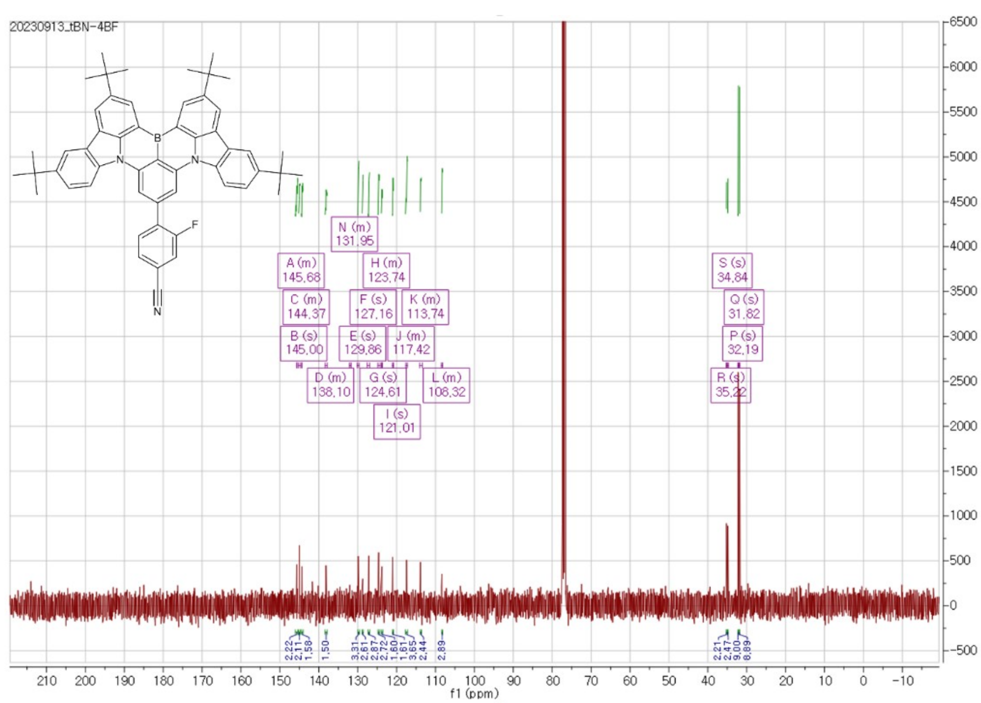

Fig. S2. [13]C-NMR of tBN-4BF

[Mass Spectrum]
Data : FAB-F566 Date : 27-Sep-2023 16:44
RT : 0.31 min Scan# : (9,16)
Elements : C 100/0, H 100/0, F 2/0, N 5/0, 10B 2/0, 11B 2/0
Mass Tolerance : 10ppm, 5mmu if m/z < 500, 10mmu if m/z > 1000
Unsaturation (U.S.) : 20.0 - 40.0

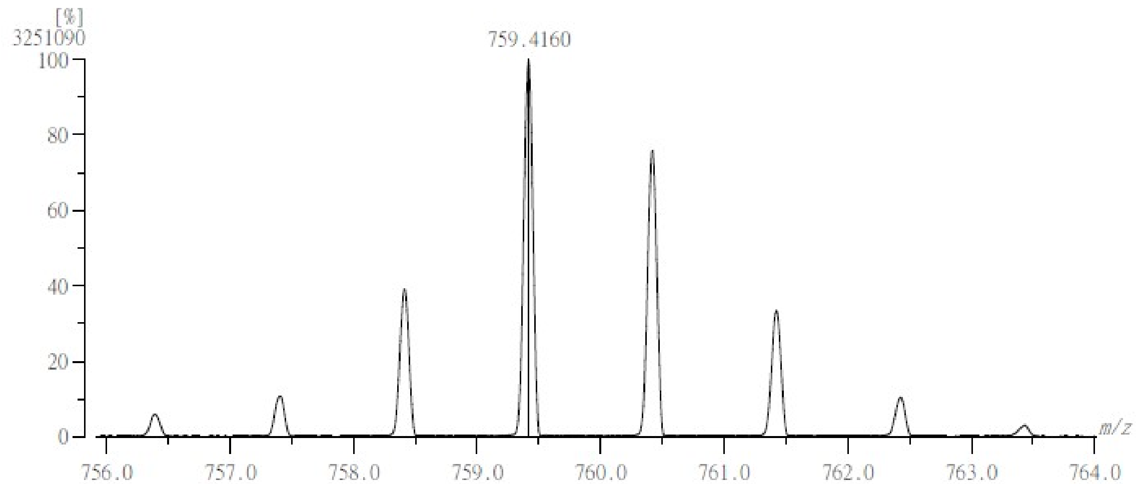

	Observed m/z	Int%	Err[ppm / mmu]	U.S.	Composition
1	759.4160	100.00	+6.0 / +4.5	30.5	C55 H52 F N2
2			+6.3 / +4.7	27.0	C50 H51 F2 N5
3			+9.5 / +7.2	30.0	C55 H51 F2 10B
4			+1.2 / +0.9	33.5	C57 H51 N 10B
5			+1.5 / +1.1	30.0	C52 H50 F N4 10B
6			+4.9 / +3.7	29.5	C52 H49 F2 N2 10B2
7			-3.3 / -2.5	33.0	C54 H49 N3 10B2
8			-0.3 / -0.2	33.5	C58 H52 11B
9			-0.0 / -0.0	30.0	C53 H51 F N3 11B
10			+3.5 / +2.6	29.5	C53 H50 F2 N 10B 11B
11			-4.8 / -3.6	33.0	C55 H50 N2 10B 11B
12			-4.5 / -3.4	29.5	C50 H49 F N5 10B 11B
13			-1.3 / -1.0	32.5	C55 H49 F 10B2 11B
14			-1.1 / -0.8	29.0	C50 H48 F2 N3 10B2 11B
15			-9.3 / -7.1	32.5	C52 H48 N4 10B2 11B
16			+7.2 / +5.5	33.0	C51 H46 N5 10B2 11B
17			+2.0 / +1.5	29.5	C54 H51 F2 11B2
18			-6.3 / -4.8	33.0	C56 H51 N 11B2
19			-6.0 / -4.6	29.5	C51 H50 F N4 11B2
20			-2.5 / -1.9	29.0	C51 H49 F2 N2 10B 11B2
21			+5.8 / +4.4	33.0	C52 H47 N4 10B 11B2
22			-7.3 / -5.6	32.0	C53 H48 F N 10B2 11B2
23			+9.2 / +7.0	32.5	C52 H46 F N2 10B2 11B2
24			-7.1 / -5.4	28.5	C48 H47 F2 N4 10B2 11B2
25			+9.5 / +7.2	29.0	C47 H45 F2 N5 10B2 11B2

Fig. S3. GC-HRMS of tBN-4BF

- **Device structure**

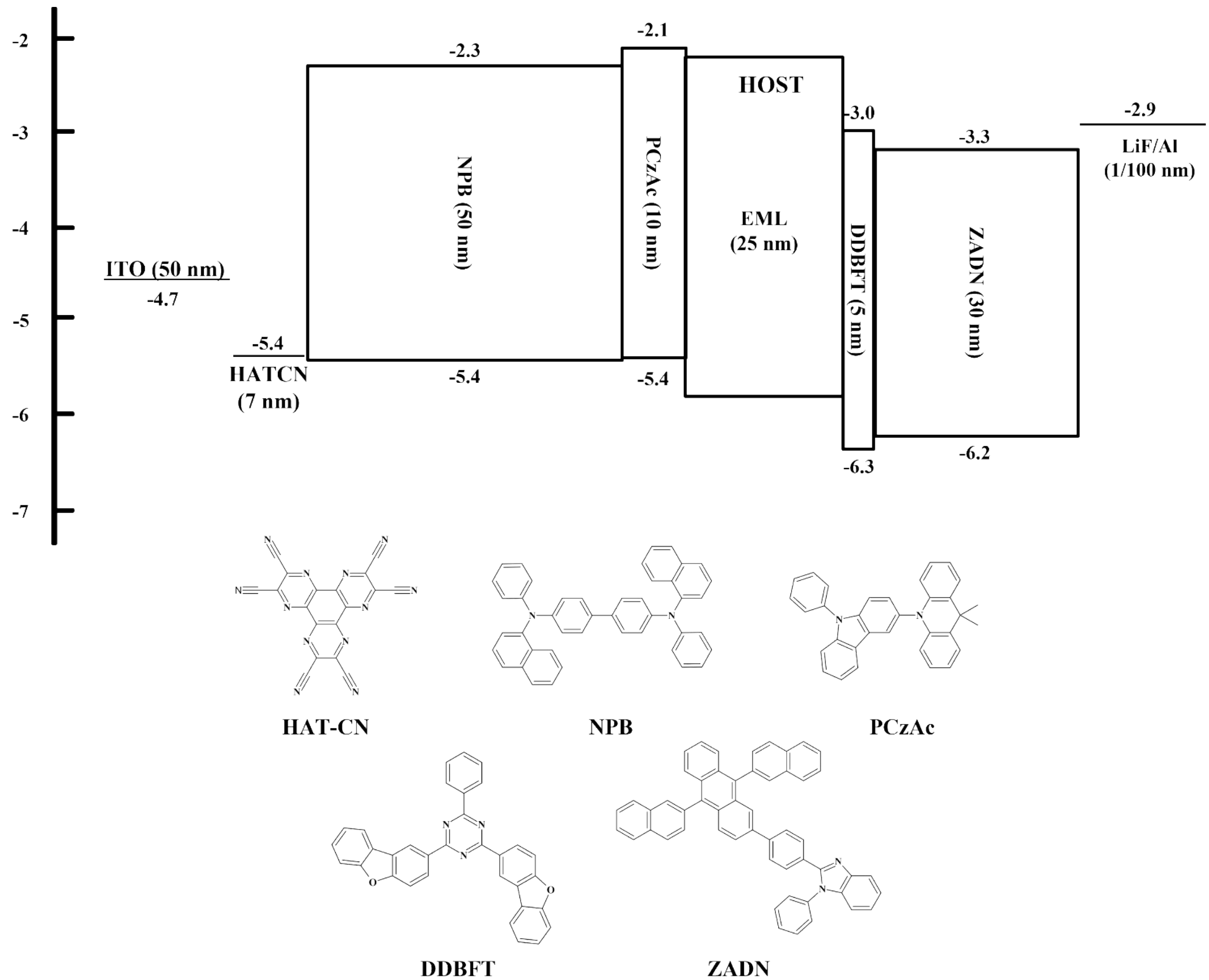

Fig. S4. Energy level diagram in Device A.

In this work, 1, and 3 wt% doped tBN-4BF device were prepared with Device A which TADF sensitizer is 0 wt%, and HF device were prepared with Device A which TADF sensitizer is 20 wt% ;

Where EML is composed of;

Device A1 : 4CzIPN + tBN-4BF 1 wt%

Device A2 : 4CzIPN + tBN-4BF 3 wt%

Device A3 : TCz-4mCNTrz + tBN-4BF 1 wt%

Device A4 : TCz-4mCNTrz + tBN-4BF 3 wt%

Device A: To investigate the lifetimes performance of the 4CzIPN and TCz-4mCNTrz we fabricated the device with structure of ITO (50 nm) / HAT-CN (7 nm) / NPB (10 nm) / PCzAC (10 nm) / PIC-Trz + TADF sensitizer (0, 20 wt%) + tBN-4BF(1, 3 wt%) (20 wt%) (25 nm) / DDBFT (5 nm) / ZADN (40 nm) / LiF (1 nm) / Al (100 nm). In these devices, 1,4,5,8,9,11-Hexaazatriphenylenehexacarbonitrile (HAT-CN) as hole-injecting layer (HIL), *N*,*N′*-Di(1-naphthyl)-*N*,*N′*-diphenyl-(1,1′-biphenyl)-4,4′-diamine (NPB) as hole-transporting layer (HTL), 9,10-Dihydro-9,9-dimethyl-10- (9-phenyl-9*H*-carbazol-3-yl)-acridine (PCzAC) as electron-blocking layer (EBL), 2,4-Bis(dibenzo[*b*,*d*]furan-2-yl)-6-phenyl-1,3,5-triazine (DDBFT) as hole-blocking layer (HBL), and 2,2,2″2-[4-(9,10-Di-naphthalen-2-yl-anthracen-2-yl)-phenyl]-1-phenyl-1*H*-benzoimidazole (ZADN) as electron-transporting layer (ETL).

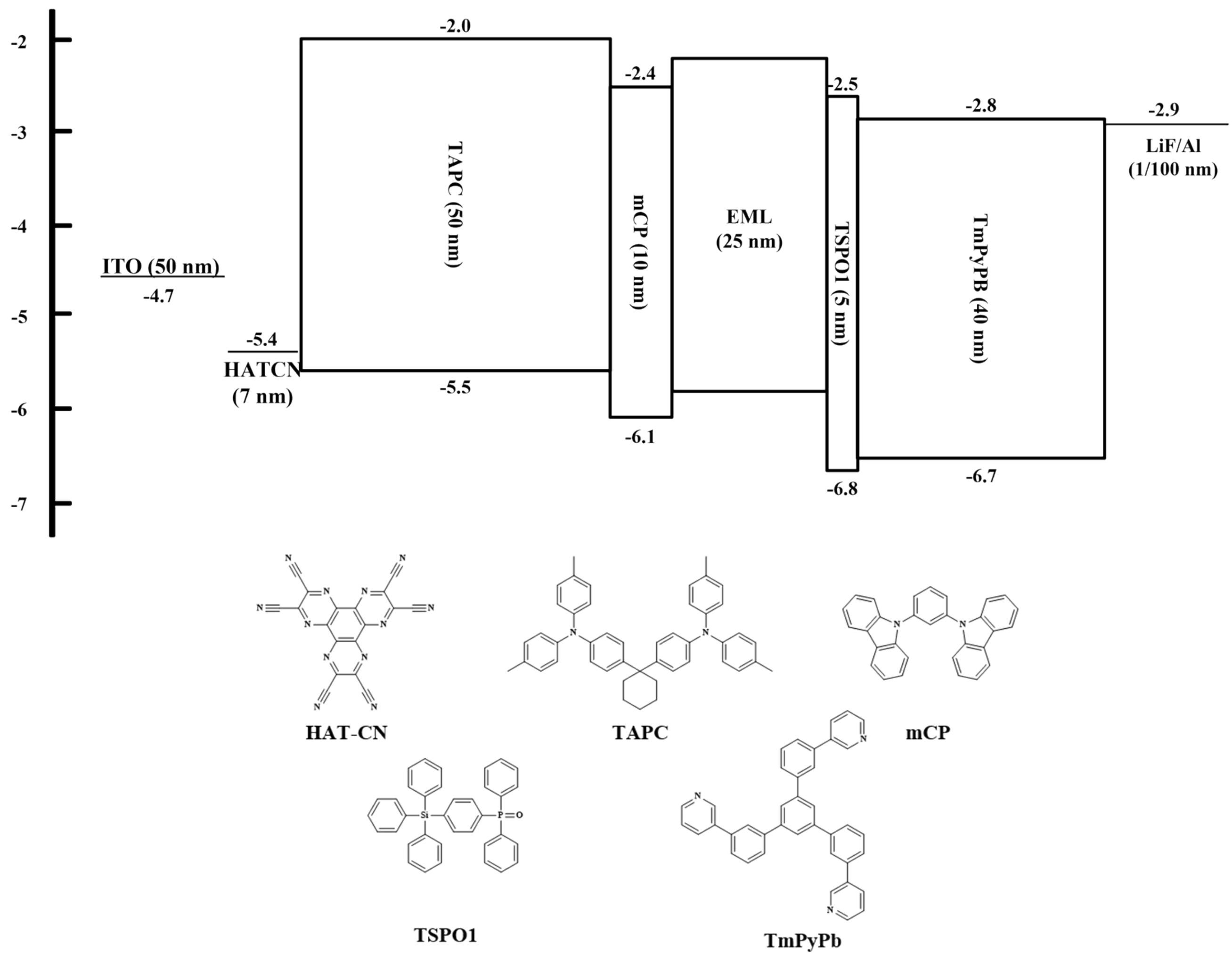

Fig. S5. Energy level diagram in Device B.

Device B: To investigate the efficiency device performance of the TCz-2mCNTrz, TCz-4mCNTrz and TCz-pCNTrz, we fabricated the device with structure of ITO (50 nm) / HAT-CN (7 nm) / TAPC (50nm) / mCP (10 nm) / PIC-Trz + TADF sensitizer (20 wt%) + tBN-4BF(1, 3 wt%) (25 nm) / TSPO1 (5 nm) / TmPyPB (40 nm) / LiF (1 nm) / Al (100 nm). In these devices, 1,4,5,8,9,11-Hexaazatriphenylenehexacarbonitrile (HAT-CN) as hole-injecting layer (HIL), 4,4′-Cyclohexylidenebis[*N*,*N*-bis(4-methylphenyl)benzenamine] (TAPC) as hole-transporting layer (HTL), 1,3-bis(9*H*-carbazolyl)benzene (mCP) as electron-blocking layer (EBL), diphenyl[4-

(triphenylsilyl)phenyl]phosphine oxide (TSPO1) as hole-blocking layer (HBL), and 2,2′,2″ 1,3,5-Tris(3-pyridyl-3-phenyl)benzene (TmPyPB) as electron-transporting layer (ETL).

Where EML is composed of;

Device B1 : TCz-4mCNTrz + tBN-4BF 1 wt%

Device B2 : TCz-4mCNTrz + tBN-4BF 3 wt%

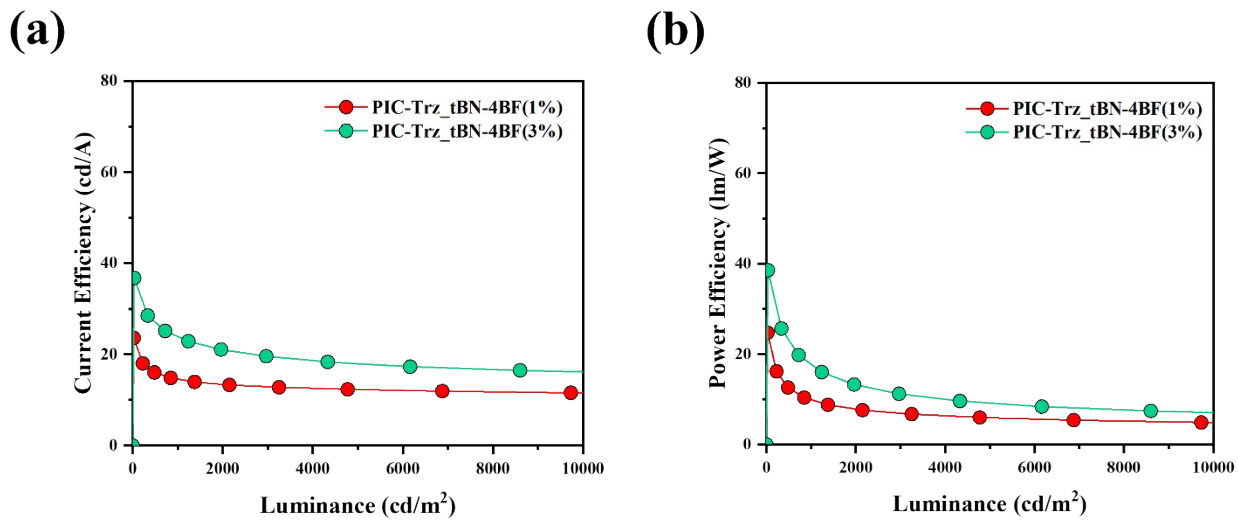

Fig. S6. Device performance of 1, 3 wt% tBN-4BF doped in PIC-Trz (a) The CE - Luminance curves (b) The PE – Luminance curves.

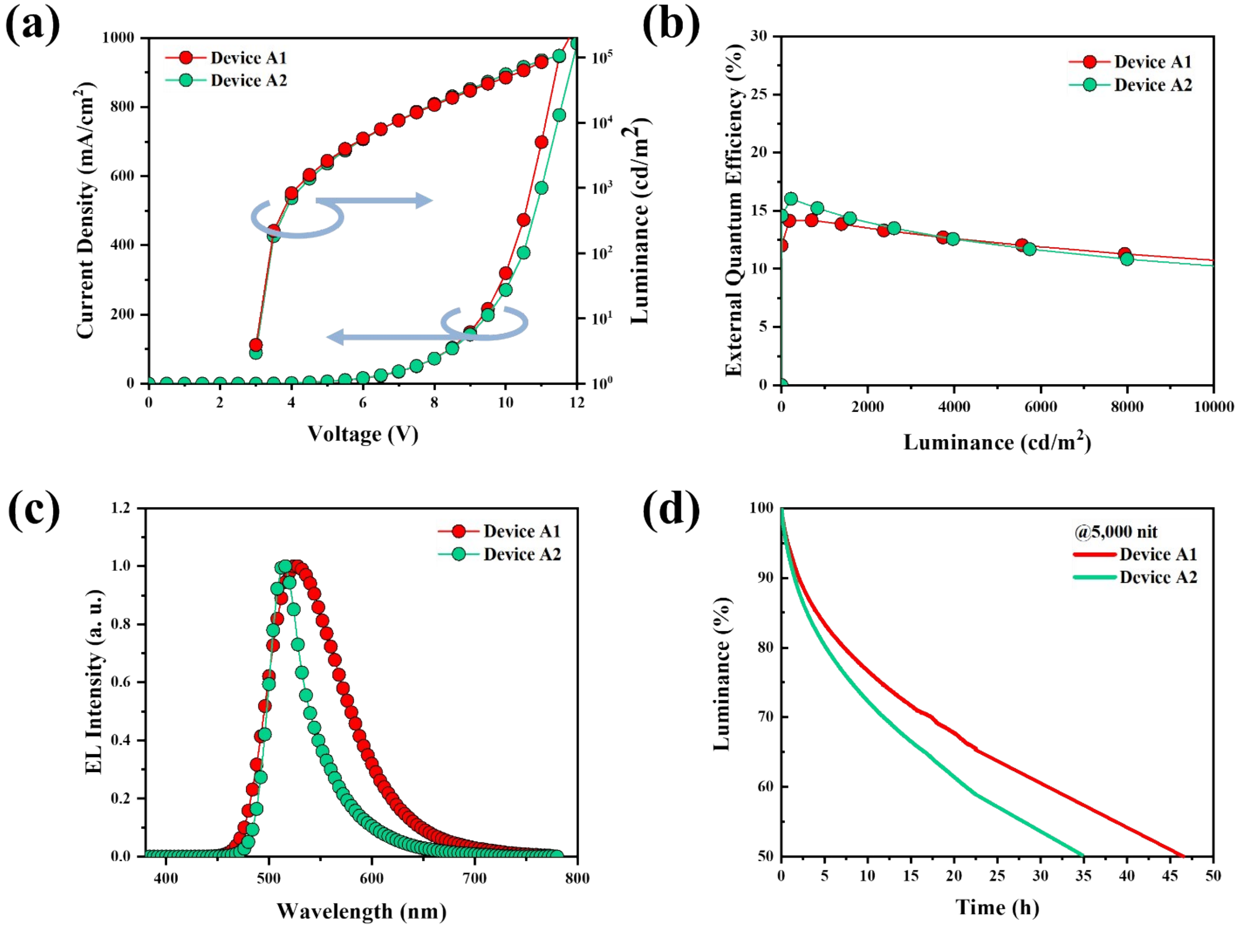

Fig. S7. Device performance of HF device(where TADF sensitizer is 4CzIPN with Device A) (a) The current density-voltage-luminance (J-V-L) curves (b) The EQE-Luminance-Current efficiency curves (c) Normalized EL intensities at the current density of 1,000 nit (d) device lifetime curves at an initial luminance 5,000 nit.

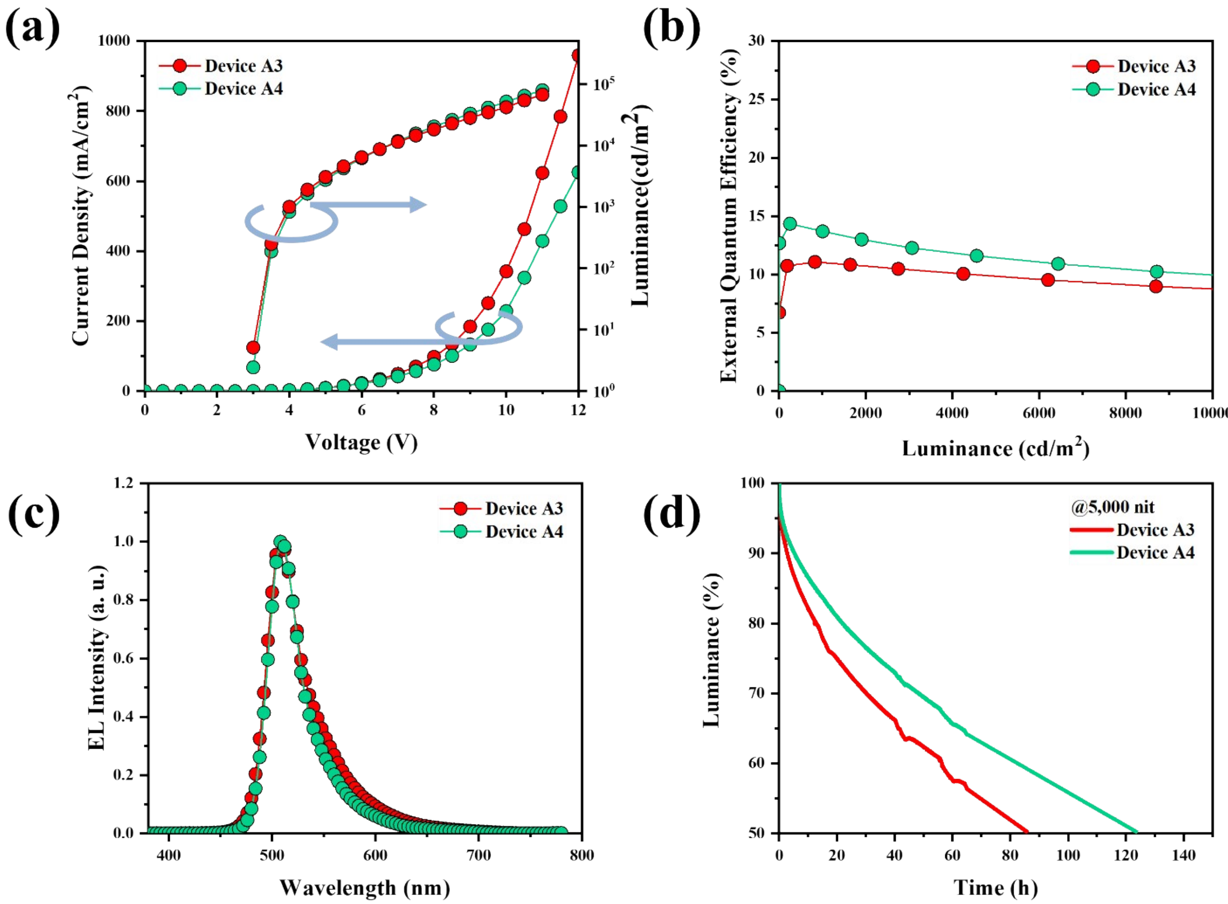

Fig. S8. Device performance of HF device(where TADF sensitizer is TCz-4mCNTrz with Device A) (a) The current density-voltage-luminance (J-V-L) curves (b) The EQE-Luminance-Current efficiency curves (c) Normalized EL intensities at the current density of 1,000 nit (d) device lifetime curves at an initial luminance 5,000 nit.

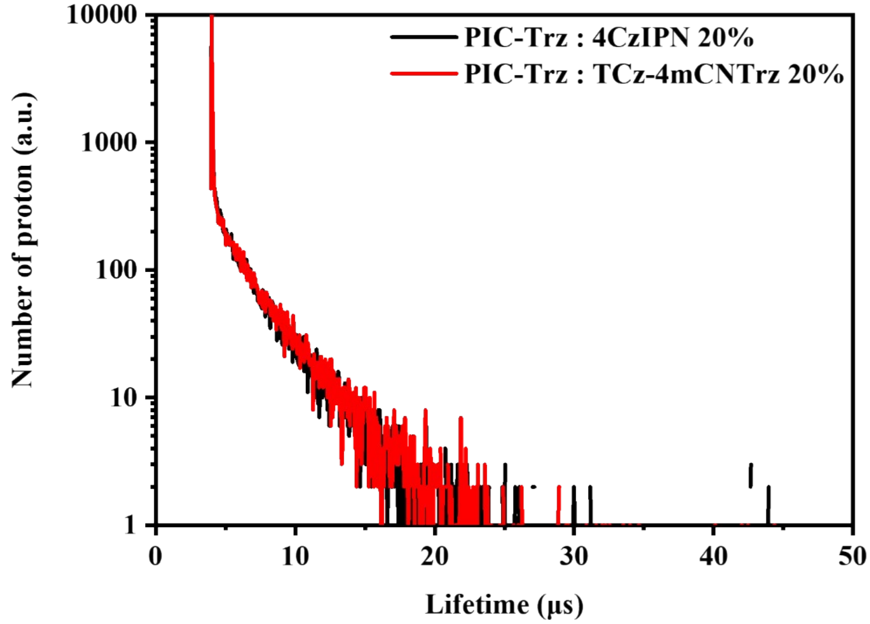

Fig. S9. Transient PL decay spectra of doped films(20 wt% doping concentration) of 4CzIPN, and TCz-4mCNTrz with PIC-Trz as the host

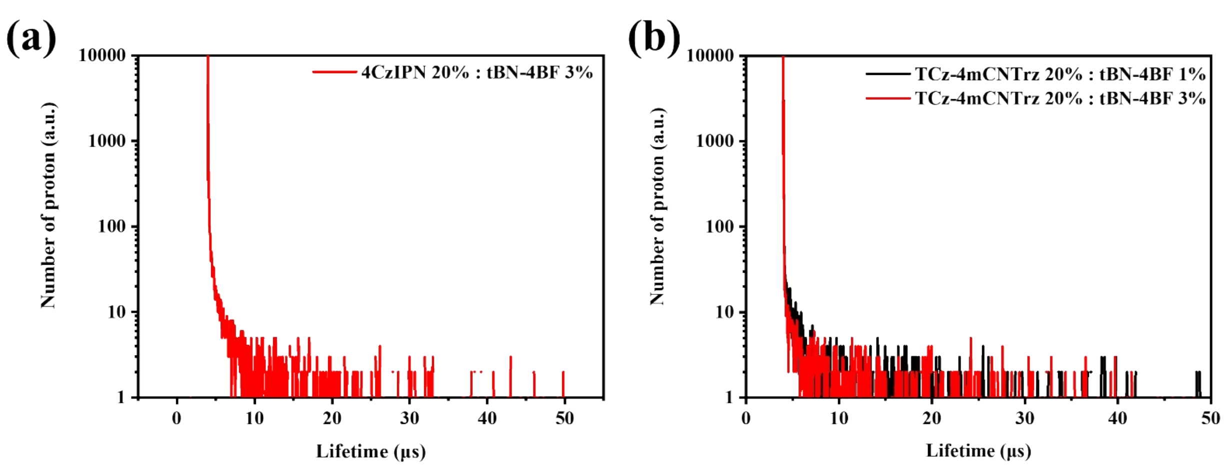

Fig. S10. Transient PL decay spectra of doped films(1, 3 wt % of tBN-4BF and 20 wt% of TADF sensitizer with PIC-Trz as the host)

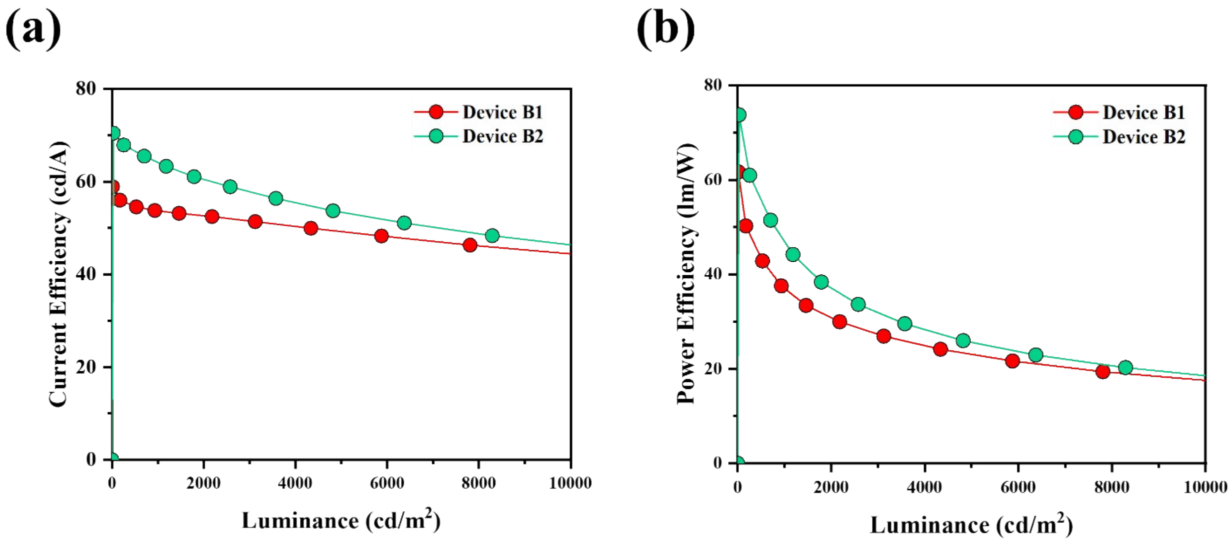

Fig. S11. Device performance of Device B1~2 (a) The CE - Luminance curves (b) The PE – Luminance curves.

Table S1. Transient PL properties of doped film of tBN-4BF with PIC-Trz host.

Material	τ_p (ns)[a]	τ_d (μs)[b]	A_1[c]	A_2[d]	Total
1 wt%	9.00	5.30	15745.1	14540.9	30295.5
3 wt%	11.0	3.86	17997.3	12094.5	30094.1

[a]Prompt fluorescence lifetime of the TADF materials; [b]Delayed fluorescence lifetime of the TADF materials; [c]Prompt components of integrating the transient PL curves; [d]Delayed components of integrating the transient PL curves

Table S2. PLQYs and transient PL properties of dopoed film of 4CzIPN and TCz-4mCNTrz with PIC-Trz host.

Material	τ_p (ns)[a]	τ_d (μs)[b]	Φ_{Total} (%)	Φ_F (%)[c]	Φ_{TADF} (%)[d]	k_P (10^7	k_D (10^5	k_r^S (10^7	k_{nr}^T (10^5	k_{ISC} (10^7	k_{RISC} (10^5 s^{-1})[j]

						s^{-1})$^{(e)}$	s^{-1})$^{(f)}$	s^{-1})$^{(g)}$	s^{-1})$^{(h)}$	s^{-1})$^{(i)}$	
4CzIPN	36.6	2.69	95.5	51.0	40.2	2.73	3.71	1.39	0.66	1.33	5.98
TCz-4mCNTrz	29.1	2.55	90.3	56.6	25.0	3.43	3.92	1.94	1.66	1.49	3.98

[a]Prompt fluorescence lifetime of the TADF materials; [b]Delayed fluorescence lifetime of the TADF materials; [c]Prompt components of the PLQYs were calculated by integrating the transient PL curves; [d]Delayed components of PLQYs; [e]Rate constant of prompt components; [f]Rate constant of delay components; [g]Radiative decay rate; [h]Nonradiative decay rate; [i]Rate constants for ISC; [j]Rate constants for RISC

Table S3. Transient PL properties of doped film of 4CzIPN and TCz-4mCNTrz **with PIC-Trz host.**

Material	τ_p (ns)$^{(a)}$	τ_d (μs)$^{(b)}$	$A_1^{(c)}$	$A_2^{(d)}$	Total
4CzIPN	36.6	2.69	30346.4	26356.4	56850.1
TCz-4mCNTrz	29.1	2.55	44021.8	26101.5	70273.3

[a]Prompt fluorescence lifetime of the TADF materials; [b]Delayed fluorescence lifetime of the TADF materials; [c]Prompt components of integrating the transient PL curves; [d]Delayed components of integrating the transient PL curves

Table S4. PLQYs and transient PL properties of Device A2~4.

Film	TADF senitizer ratio (wt%)	tBN-4BF ratio (wt%)	$\tau^{HF}{}_p$ (ns)$^{(a)}$	$\tau^{HF}{}_d$ (μs)$^{(b)}$	Φ_{Total} (%)
Device A2	4CzIPN	3	13.5	0.35	90.3

Device A3	TCz-4mCNTrz	1	11.4	0.49	97.9
Device A4	TCz-4mCNTrz	3	11.9	0.81	95.5

[a]Prompt fluorescence lifetime of the TADF materials; [b]Delayed fluorescence lifetime of the TADF materials.

Table S5. FRET and DET calculation summary between TADF sensitizer(4CzIPN, and TCz-4mCNTrz), and tBN-4BF.

Film	TADF senitizer ratio (wt%)	tBN-4BF ratio (wt%)	J (10^{-25} m^2)$^{(a)}$	R_0 (nm)$^{(b)}$	Φ_{FET} (%)$^{(c)}$	k_{FET} (10^7 s^{-1})$^{(d)}$	k_{DET} (10^6 s^{-1})$^{(e)}$
Device A2	4CzIPN	3	7.28	3.99	53.6	3.97	23.7
Device A3	TCz-4mCNTrz	1	5.68	3.82	68.8	6.03	14.6
Device A4	TCz-4mCNTrz	3	5.68	3.82	67.4	5.67	6.64

[a]Overlap integral between the UV-vis spectra of tBN-4BF and PL spectra of all TADF sensitizers; [b]Förster energy transfer radii; [c]Efficient of Förster energy transfer;[d]Rate constants for Förster energy transfer; [e]Rate constant of Dexter energy transfer.

Table S6. The weakest bond dissociation energy values of calculated at anion, and cation state for 4CzIPN, and TCz-4mCNTrz.

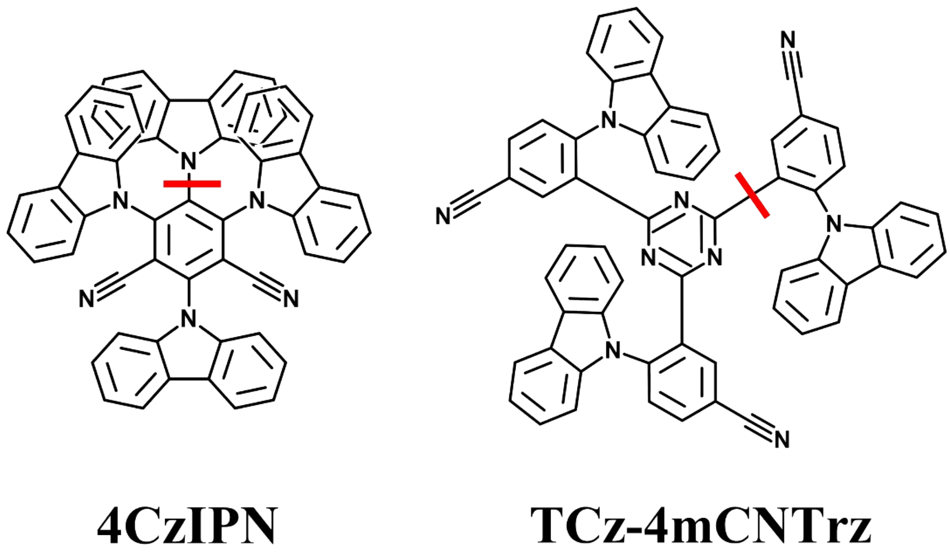

TADF materials	Anion BDE (eV)	Cation BDE (eV)	Ref.
4CzIPN	1.78	3.87	[7]
TCz-4mCNTrz	3.15	4.17	[8]

- **Equation**

The rate constants of ISC(k_{ISC}) and RISC(k_{RISC}) of tBN-4BF based on the following equations [1-3] :

$$k_p = 1/\tau_p \quad (1)$$

$$k_r^S = \Phi_p/k_p \quad (2)$$

$$k_{TADF} = 1/\tau_d \quad (3)$$

$$k_{nr}^T = k_{TADF} - \Phi_p \times k_{RISC} \quad (4)$$

$k_{ISC} = (1- \Phi_p) / \tau_p$ ···(5)

$k_{RISC} = (k_p \times k_{TADF} \times \Phi_{TADF})/(k_{ISC} \times \Phi_p)$ ···(6)

where, k_P is rate of prompt components, k_{TADF} is rate of delay components, k_r^s is rate of radiative decay on the singlet excited state to ground state, k_{nr}^T is rate of non-radiative decay on the triplet excited state to ground state, k_{ISC} is rate of ISC, k_{RISC} is rate of RISC, Φ_p is prompt PLQY, and Φ_{TADF} is delayed PLQY.

Eq. S1. Exciton Lifetime and Rate Constant equation.

By assuming (i) $k_{PF} \gg k_{DF}$ and (ii) (k_r^S, k_{ISC} and k_{FET}) ≫ (k_{nr}^S, k_r^T, k_{nr}^T and k_{DET}), the average k_{FET} and k_{DET} can be calculated by Eq. S2 (5), (6), and (7);

$R_0 = [(9(\text{In}10)k^2\Phi_{TADF}) \times J/(128\pi^5 N_A \eta^4)]^{1/6}$ ···(1)

$\Phi_{FRET} = 1-(\tau^{HF}{}_p/\tau^{TADF}{}_p)$ ··(2)

$k_{FRET} = \Phi_{FRET}/\tau^{HF}{}_p$ ··(3)

$k_{DET} = 1/ \tau^{HF}{}_d - 1/ \tau_d + k_{RISC} \times k_{ISC} \times (\tau^{HF}{}_p - \tau_p)$ ··(4)

where, k^2 is the dipole-dipole interaction(in this study 2/3 was used which is the value for a random distribution), N_A is the Avogadro constant, η is the refractive index of the film.[4-6]

Eq. S2. Equation of Förster energy transfer radius and rate constant of Förster resonance energy transfer.

◆ Reference

[1] R. Pei, J. Lou, G. Li, H. Liu, X. Yin, C. Zhou, Z. Wang, and C. Yang, *Chemical Engineering Journal* **2022**, 437, 135222

[2] J. Huang, H. Nie, J. Zeng, Z. Zhuang, S. Gan, Y. Cai, J. Guo, S. Su, Z. Zhao, and B. Z. Tang, *Angew. Chem. Int. Ed* **2017**, 56, 12971-12976

[3] D. Zhou, G. S. M. Tong, G. Chen, Y. Tang, W. Liu, D. Ma, L. Du, J. Chen, and C. Che, *Adv. Mater.* **2022**, 34, 2206598

[4] W. Xie, X. Peng, M. Li, W. Qiu, W. Li, Q. Gu, Y. Jiao, Z. Chen, Y. Gan, K. K. Liu, and S. su, *Adv. Optical Mater.* **2022**, 10, 2200665

[5] K. Stavrou, L. G. Franca, A. Danos, and A. Monkman, *Chemrxiv*. **2023**, "Understanding the Key Requirements for Ultra-Efficient Sensitisation in Hyperfluorescence OLEDs."

[6] J. Liu, J. Liu, H. Li, Z. Bin, and J. You, Angew. Chem. Int. Ed. **2023**, 62, e202306471

[7] Y. H. Jung, D. Karthik, H. Lee, J. H. Maeng, K. J. Yang, S. Hwang, and J. H. Kwon, *ACS Appl. Mater. Interfaces* **2021**, 13, 17882-17891

[8] J. Yoo, Y. Choi, K. W. Kim, T. H. Ha, and C. W. Lee, *Dyes and Pigments* **2023**, 214, 111200